BioMedInformatics

MDPI

Article

Omicron SARS-CoV-2 Spike-1 Protein's Decreased Binding Affinity to α7nAChr: Implications for Autonomic Dysregulation of the Parasympathetic Nervous System and the Cholinergic Anti-Inflammatory Pathway—An In Silico Analysis

Domiziano Doria [1], Alessandro D. Santin [2], Jack Adam Tuszynski [1,3,*], David E. Scheim [4] and Maral Aminpour [5]

[1] DIMEAS, Politecnico di Torino, Corso Duca degli Abruzzi 24, 10129 Torino, Italy
[2] Obstetrics, Gynecology & Reproductive Sciences, Yale School of Medicine, New Haven, CT 06520-8063, USA
[3] Department of Physics, University of Alberta, Edmonton, AB T6G 1Z2, Canada
[4] US Public Health Service, Commissioned Corps, Inactive Reserve, Blacksburg, VA 24060, USA
[5] Department of Biomedical Engineering, University of Alberta, Edmonton, AB T6G 1Z2, Canada
* Correspondence: jackt@ualberta.ca

Abstract: Omicron is the dominant strain of COVID-19 in the United States and worldwide. Although this variant is highly transmissible and may evade natural immunity, vaccines, and therapeutic antibodies, preclinical results in animal models and clinical data in humans suggest omicron causes a less severe form of infection. The molecular basis for the attenuation of virulence when compared to previous variants is currently not well understood. Using protein–ligand docking simulations to evaluate and compare the capacity of SARS-CoV-2 spike-1 proteins with the different COVID-19 variants to bind to the human α7nAChr (i.e., the core receptor under the control of the vagus nerve regulating the parasympathetic nervous system and the cholinergic anti-inflammatory pathway), we found that 10 out of the 14 mutated residues on the RBD of the B.1.1.529 (Omicron) spike, compared to between 0 and 2 in all previous variants, were present at the interaction interface of the α7nAChr. We also demonstrated, through protein–protein docking simulations, that these genetic alterations cause a dramatic decrease in the ability of the Omicron SARS-CoV-2 spike-1 protein to bind to the α7nAChr. These results suggest, for the first time, that the attenuated nature of Omicron infection in humans and animals compared to previous variants may be attributable to a particular set of genetic alterations, specifically affecting the binding site of the SARS-CoV-2 spike-1 protein to the α7nAChr.

Keywords: SARS-CoV-2; Alpha-7 nicotinic receptor; protein–protein docking; molecular modeling; Omicron

check for updates

Citation: Doria, D.; Santin, A.D.; Tuszynski, J.A.; Scheim, D.E.; Aminpour, M. Omicron SARS-CoV-2 Spike-1 Protein's Decreased Binding Affinity to α7nAChr: Implications for Autonomic Dysregulation of the Parasympathetic Nervous System and the Cholinergic Anti-Inflammatory Pathway—An In Silico Analysis. *Biomedinformatics* **2022**, *2*, 553–564. https://doi.org/10.3390/biomedinformatics2040035

Academic Editor: Jörn Lötsch

Received: 19 September 2022
Accepted: 22 October 2022
Published: 25 October 2022

Publisher's Note: MDPI stays neutral with regard to jurisdictional claims in published maps and institutional affiliations.

Copyright: © 2022 by the authors. Licensee MDPI, Basel, Switzerland. This article is an open access article distributed under the terms and conditions of the Creative Commons Attribution (CC BY) license (https://creativecommons.org/licenses/by/4.0/).

1. Introduction

The rapid spread of the B.1.1.529 (Omicron) SARS-CoV-2 variant, first identified in Botswana and South Africa in November 2021, raised major concerns regarding the prospect of a new global wave of lethal COVID-19 infections. Moreover, data indicating as many as 37 mutations in the Omicron spike protein relative to the Wuhan-Hu-1 strain [1] raised further concerns that this variant could evade natural immunity, vaccines, and therapeutic antibodies. Omicron has also been found to be more transmissible than previous strains (i.e., Omicron may infect and multiply 70 times faster in the upper airways than Delta) [2]. Early clinical data, however, suggest a less severe, more indolent form of infection by Omicron in humans [3–6]. Consistent with this human clinical data, in multiple recent reports, Omicron has been shown to cause milder respiratory infection in animal models and to be attenuated in both mice and hamsters for causing infection and/or disease, compared to previous variants [7,8]. Nevertheless, the molecular basis for this attenuation, with respect to previous variants in humans and rodents, is not yet well understood.

We have recently performed protein–ligand docking simulations to evaluate the potential binding sites of multiple therapeutic compounds against the SARS-CoV-2 spike-1 protein [9]. In this in silico study, in agreement with other reports [10,11], we demonstrated a potential direct binding of the SARS-CoV-2 spike-1 protein to the Alpha-7 nicotinic acetylcholine receptor (α7nAChr), which is the core receptor under the control of the vagus nerve, regulating the parasympathetic nervous system and the cholinergic anti-inflammatory pathway [12]. This study, and other studies [13], demonstrated that the spike-1 Y674-R685 region penetrates deeply into the binding pocket in which it forms interactions with the residues lining the aromatic box, namely with TrpB, TyrC1, and TyrC2 [10,11]. This motif contains a four-residue, polybasic PRRA insertion that is homologous to several neurotoxins known to target the α7nAChr, as well as several known nAChR antagonists, further suggesting that this region of the SARS-CoV-2 spike protein may bind to the α7nAChr [10,11], as well as to other receptors, including neuropilins [14]. Consistent with this view, the abrogation of the PRRA motif has been experimentally demonstrated to affects virus entry into host cells [15,16]. Importantly, the α7nAChr-regulated vagus nerve-controlled anti-inflammatory pathway is known to play a crucial role in balancing the body's response to inflammation and sepsis [12,17], connecting the involuntary parasympathetic nervous system innervating all major organs to cytokine-producing cells, such as TNF, IL-1, and IL-6-secreting macrophages, lymphocytes, and mast cells [12,17–19], which in turn play a major role during the inflammatory phase of COVID-19 infection (i.e., the cytokine storm) [20]. Because the α7nAChr is the known port of entry to the human body for other neurotropic viruses, such as the rabies virus [21], as well as the specific binding site to human neurons of multiple lethal snake venom toxins [10,11], it stands to reason that the ability of the SARS-CoV-2 spike-1 protein to bind and hijack the α7nAChr-regulated response of the autonomous nervous system to inflammation may represent one of the crucial characteristics, explaining its high lethality in both humans and animals. Clinical data correlating hypercytokinemia and hyperinflammation with the dysregulation of the Ach/α7nAChR pathway in severe COVID-19 patients further support this hypothesis [22].

Accordingly, in this study, we used protein–ligand docking simulations to evaluate and compare the capacity of SARS-CoV-2 spike-1 proteins with the different COVID-19 variants (i.e., Alpha, Beta, Gamma, Delta, and Omicron) to bind to the human α7nAChr. Notably, we found that 10 out of the 14 mutated residues on the RBD of the B.1.1.529 (Omicron) spike, compared to between 0 and 2 in all previous variants, were present at the interaction interface with the α7nAChr. We also demonstrated through protein–protein docking simulations that these genetic alterations cause a dramatic decrease in the ability of the Omicron SARS-CoV-2 spike-1 protein to bind to the α7nAChr. Clinically speaking, these results suggest that the attenuated nature of Omicron infection in humans and animals, compared to previous variants, may be attributable to a particular set of genetic alterations specifically affecting the binding site of the SARS-CoV-2 spike-1 protein to the α7nAChr.

2. Materials and Methods

2.1. Proteins Preparation

The structure of the complex between the spike (PDB: 6VSB) and α7nAChr was obtained from Aminpour et al. [9]. The atomic coordinates that activated the α7nAChr (PDB: 7KOX) were obtained from the PDB [23]. Meanwhile, the Omicron spike (B.1.1.529) crystallography structure was taken from PDB (7QO7) [24]. The Delta spike structure, finally, was obtained from PDB (7W92) [25]. All proteins were prepared in the Molecular Operating Environment (MOE, Chemical Computing Group; https://www.chemcomp.com/Products.htm, accessed on 5 September 2022) software package, with their protonation states adjusted and a physiological pH of 7 maintained. The structure was minimized also using MOE software.

Amino acid mutations of the Alpha, Beta, Gamma, Delta, and Omicron variants of SARS CoV-2, with a focus on NTD (aa 18–292) and RBD (aa 318–513) segments, were reproduced from Aminpour et al. [9] as listed in Table 1.

Table 1. The different mutations for selected SARS-CoV-2 variants.

B.1.1.7	**B.1.351**	**P.1**	**B.1.617.2**
(United Kingdom, Alpha)	(South Africa, Beta)	(Brazil, Gamma)	(India, Delta)
H69-V70 deletion (NTD) Y144 deletion (NTD) N501Y (RBD)	L18F (NTD) D80A (NTD) D215G (NTD) 242–244 deletion (NTD) R2461 (NTD) K417N (RBD) E484K (RBD) N501Y (RBD)	L18F (NTD) T20N (NTD) P26S (NTD) D138Y (NTD) R190S (NTD) K417T (RBD) E484K (RBD) N501Y (RBD)	T19R (NTD) 157–158 Deletion (NTD) L452R (RBD) T478K (RBD)
B.1.1.529 (Omicron)			
A67V (NTD) H69-V70 deletion (NTD) T95I (NTD) G142D (NTD) V143-Y144-Y145 deletion (NTD) N211I (NTD) L212V (NTD) E214-P215-E216 addition (NTD) G339D (RBD) S371L (RBD) S373P (RBD) S375F (RBD) K417N (RBD) N440K (RBD) G446S (RBD) S447N (RBD) T478K (RBD) E484A (RBD) Q493R (RBD) G496S (RBD) Q498R (RBD) N501Y (RBD)			

2.2. Contact Analysis

Considering the complex between the main spike protein and α7nAChr, all of the interactions involved in the binding of the two structures were analyzed using the MOE software and particularly its "Contacts" analysis function, as this tool provides information about the bond type and the interacting residues involved.

The interaction between the two proteins was evaluated using six types of contacts: hydrogen bonds (H) relative to hydrogen bond contacts; metal, relative to metal interactions which are bonded, or are close enough to be within bonded distance; ionic, for ionic bonds; arene, for arene interactions, including π:π, π-H, and π:cation contacts; covalent, relative to covalent bonds; and distance (D) interactions, relative to van der Waals distance interactions. Once these features had been extracted, we compared all of the residues involved in this bond to those involved in other variants' mutations in order to ascertain which amino acid will mutate and what the corresponding variant was. This method allowed us to determine whether the contact between the spike protein and α7nAChr modified the interaction, as well as which variant was driving these changes and which residues were involved.

2.3. Protein–Protein Docking

PatchDock software was used to perform protein–protein docking simulations [26,27]. PatchDock, it should be noted, is a geometry-based molecular docking algorithm using shape complementarity principles. The algorithm first computed the molecular surface of the proteins, then performed a segmentation to detect geometric patches (concave, convex, and flat surface pieces). Then, in the surface-match-patching step, the complementary patches were selected in order to generate candidate transformations. The candidate transformations from the previous step were evaluated using a scoring function, taking

into account both geometric fit and solvation energy. The geometrically unacceptable presentations of the atoms of complex structures were filtered. Finally, an RMSD (root mean square deviation) clustering method was applied to the remaining candidates to discard similar and redundant structures. Considering the size of the proteins, we used a clustering RMSD of a 4.0 Å arm for all of the protein–protein docking analyses. The results obtained from PatchDock were further refined with the associated server, FireDock, which delivers a refinement of both the score function and the complex geometries.

The final structures were visualized and validated before the final representation was created, with the candidate complex in terms of lipophilicity and attachment to the α7nAChr, as well as with minimal binding energy, being selected in order to ensure that the states with the optimal features for every single complex were reflected in the final results. All references to the energy states are as specified in Table 2.

Table 2. The different features that define the energy states associated with the interactions between the different spike proteins and the α7nAChr.

Glob	Global Energy, the Binding Energy of the Solution
aVdW	attractive van der Waals energy
rVdW	repulsive van der Waals energy
ACE	atomic contact energy (ACE)

2.4. Align Complexes

After we obtained the different final structures, we proceeded to align these different poses. An alignment, or 'sequence alignment', is a way of arranging the primary sequences of our proteins to identify regions of similarity that may be a consequence of functional or structural relationships between the sequences. We used this instrument using MOE software to be able to align α7nAChr residues for all the 3 complexes, and this enabled us to investigate the interaction interface of all 3 variants of the COVID spike protein, demonstrating how they attach themselves individually to an α7nAChr protein. Previous simulations were performed with the same α7nAChr structure; hence, the present alignment procedure was expected to provide a consistent match between α7 and the 3 variants of the spike protein with the same position and orientation in their unique complexes.

3. Results

We first analyzed the interacting residues between the main spike protein (PDB:6VSB) and α7nAChr (PDB:7KOX), using contact analysis of MOE software. The summary of the interacting residues is presented in Table 3.

Table 3. All residues involved in the bond between the α7nAChr (PDB:7KOX) and the original SARS-CoV-2 spike protein (PDB:6VSB), with bond type interactions: distance (D), hydrogen bond (H), and ionic (I). Set A refers to α7nAChr, set B refers to spike protein. The explanation of each feature in the bond type column is described in computational details (contact analysis).

Bond Type	Set A	Set B	Bond Type	Set A	Set B	Bond Type	Set A	Set B
DH	Asn23	Arg403	D	Ser69	Ala372	D	Val68	Ser373
DH	Asp156	Thr500	D	Ser69	Trp436	D	Glu9	Phe486
D	Val68	Trp436	D	His62	Gln493	D	Pro72	Ser371
D	Phe2	Phe456	D	Glu1	Tyr489	D	Lys191	Lys444
I	Ser25	Arg403	D	Pro27	Asn501	D	Asn13	Gly485
D	Phe186	Thr500	D	Asn67	Gly339	D	Leu28	Gln498
D	Trp153	Pro499	D	Val68	Phe342	D	Phe2	Leu455
D	Arg4	Phe486	D	Lys191	Pro499	D	Thr29	Gly447
D	Phe186	Val445	D	Lys12	Glu484	D	Ser25	Tyr505
DH	Ala22	Gln493	D	His62	Leu492	D	Tyr71	Phe486
D	His62	Leu452	D	Gln26	Gln498	D	Ser69	Phe374

Table 3. *Cont.*

Bond Type	Set A	Set B	Bond Type	Set A	Set B	Bond Type	Set A	Set B
D	Phe2	Ala372	D	Asp156	Gln498	D	Tyr31	Gly446
D	Leu28	Gly446	D	Asn23	Tyr453	D	Leu28	Tyr449
D	Ser69	Phe342	D	Pro27	Tyr449	D	Ser112	Thr345
D	Asn67	Phe342	D	Val30	Val445	D	His62	Ser494
D	Trp153	Asn439	D	Thr60	Lys444	D	Pro27	Gln498
D	Leu6	Phe486	D	Tyr63	Gln493	DH	Thr29	Gln498
D	Lys8	Gly485	D	Val68	Ser371	D	Gln158	Val445
D	Glu70	Val367	D	Lys191	Ser443	D	Thr60	Tyr449
D	Lys75	Ser438	D	Tyr71	Ser371	D	Pro72	Ser373
D	Asn23	Ser494	D	Thr60	Gly446	D	Pro72	Ala372
D	Asn110	Asn440	D	Gln65	Tyr449	D	Lys12	Val483
D	Lys75	Asn439	D	Asp156	Val445	D	Glu1	Gln493
D	Lys5	Tyr489	D	Asn23	Tyr495	D	Lys8	Phe486
D	Lys75	Asn440	D	Thr29	Tyr449	DH	Thr29	Gly446
D	Asn23	Tyr505	D	Ser69	Asn343	D	Ser69	Ser373
D	Gln26	Gly496	D	Val30	Gly446	D	Tyr31	Val445
D	His62	Tyr449	D	Lys191	Val445	D	Ala22	Ser494
D	Gln158	Thr500	D	Val21	Tyr449	D	Asn13	Glu484
D	Phe2	Ser371	D	Val68	Asn343	D	Lys5	Asn487
D	Trp66	Asn343	D	Glu70	Ser373	D	Gln26	Tyr505
D	Lys75	Asn437	D	Tyr31	Lys444	D	Glu1	Phe456
D	Ser112	Leu441	D	Asn13	Val483	D	Lys5	Phe486
D	Thr29	Lys444	D	Asn23	Gly496	D	Glu1	Leu455
D	Phe2	Phe486	D	Ala22	Tyr449	D	Thr29	Val445
D	Thr60	Gly447	D	Gln26	Asn501	D	Ser69	Ser371
D	Ser111	Leu441	D	Glu70	Ser371	D	Asn67	Asn343
D	Pro20	Tyr449	D	Ala22	Tyr495			

First, we compared the interacting residues between the main spike protein (Table 3) and the mutated residues in different spike variants (Table 1). In this manner it was determined that only two residues in the Beta (E484K, N501Y), two in the Gamma (E484K, N501Y), one in the Alpha (N501Y), and none in the Delta variant were mutated. On the other hand, 33 mutations were found in the binding area between the spike and the α7nAChr in the Omicron variant. The mutated residues are summarized in Table 4 and represented in Figure 1.

Second, we performed the ulterior protein–protein docking analysis to determine the energy states of different complex 'spike variant-α7nAChr' cases. After searching configurations, scoring, filtering, and refining with FireDock software, the candidate complex was selected. Any structure, it should be noted, has a characteristic energy state that provides details about the bond and, in particular, its strength. The best docked structure was selected on the basis of its global energy. This value is considered to be related to binding free energy (Kcal/mol), and a higher negative value represents stronger binding. The details of the interaction energies between different complex 'spike variant-α7nAChr' cases are summarized in Table 5. These final predicted structures for each variant of spike protein in complex with the α7nAChr are represented in Figure 2A–C, respectively.

The α7-Delta's spike was found to have the lowest global energy (the strongest binding affinity), whereas α7-Omicron's spike was found to have the highest global energy (the weakest binding affinity). A visual inspection of the ACE feature confirmed the trend in which the impairment of the bond involving α7-Omicron, compared to α7-Delta, resulted in a lower binding energy (a stronger bond), compared to a higher one (a weaker bond).

In the last instance, the Align tool in MOE provided a graphical representation of the interaction's interface regarding the three different spikes and the α7nAChr, as shown in Figure 3. We noticed that Omicron and Delta shared a large portion of the interaction interface with α7.

Table 4. Interacting residues involved in the bond between the α7nAChr and the main SARS-CoV-2 spike protein that are mutated in the Omicron variant. Set A refers to the α7nAChr, set B refers to the original spike protein and set B-mutated refers to the mutated residues in the Omicron variant.

Set A	Set B	Set B-Mutated	Set A	Set B	Set B-Mutated
Ala22	Gln493	Q493R	Glu70	Ser373	S373P
Leu28	Gly446	G446S	Asn23	Gly496	Q493R
Asn110	Asn440	N440K	Gln26	Asn501	N501Y
Lys75	Asn440	N440K	Glu70	Ser371	S371L
Gln26	Gly496	G496S	Val68	Ser373	S373P
Phe2	Ser371	S371L	Pro72	Ser371	S371L
His62	Gln493	Q493R	Leu28	Gln498	Q498R
Pro27	Asn501	N501Y	Tyr31	Gly446	G446S
Asn67	Gly339	G339D	Pro27	Gln498	Q498R
Lys12	Glu484	E484A	Thr29	Gln498	Q498R
Gln26	Gln498	Q498R	Pro72	Ser373	S373P
Asp156	Gln498	Q498R	Glu1	Gln493	Q493R
Tyr63	Gln493	Q493R	Thr29	Gly446	G446S
Val68	Ser371	S371L	Ser69	Ser373	S373P
Tyr71	Ser371	S371L	Asn13	Glu484	E484A
Thr60	Gly446	G446S	Ser69	Ser371	S371L
Val30	Gly446	G446S			

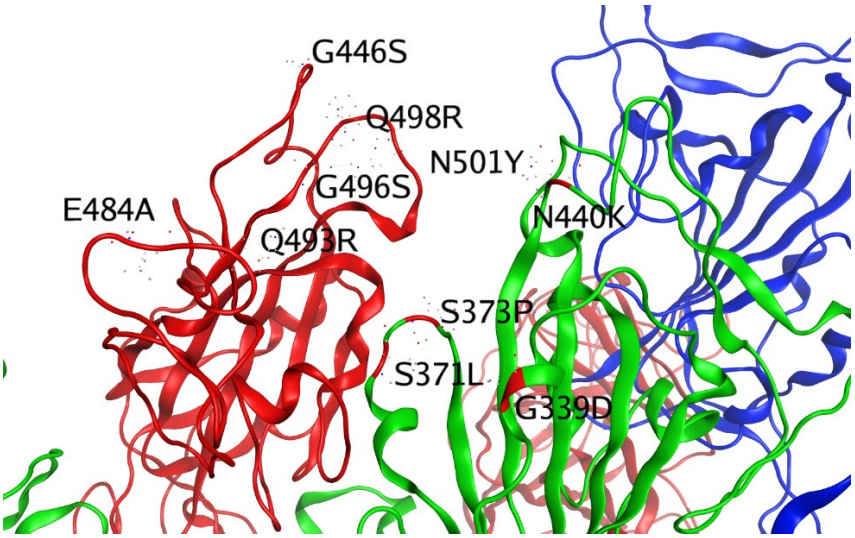


Figure 1. The residues involved in the interaction between the mutated spike protein and the α7nAChr protein in the Omicron variant. To focus on the mutations, the main spike protein is isolated in the figure. The three different isomers are presented in red, green, and blue, and we highlight how the residues mutate in the Omicron variant.

Table 5. The energy state of the bond between the α7nAChr and (A) main spike, (B) Delta, and (C) Omicron variants of spike protein. The explanation of each energy feature in the first row is described in Table 2.

Complex	Glob (Kcal/mol)	aVdW (Kcal/mol)	rVdW (Kcal/mol)	ACE (Kcal/mol)
α7-main spike	−2.45	−31.08	18.5	13.58
α7-Delta's spike	−13.05	−20.71	6.39	11.04
α7-Omicron's spike	4.84	−23.29	8.39	14.41

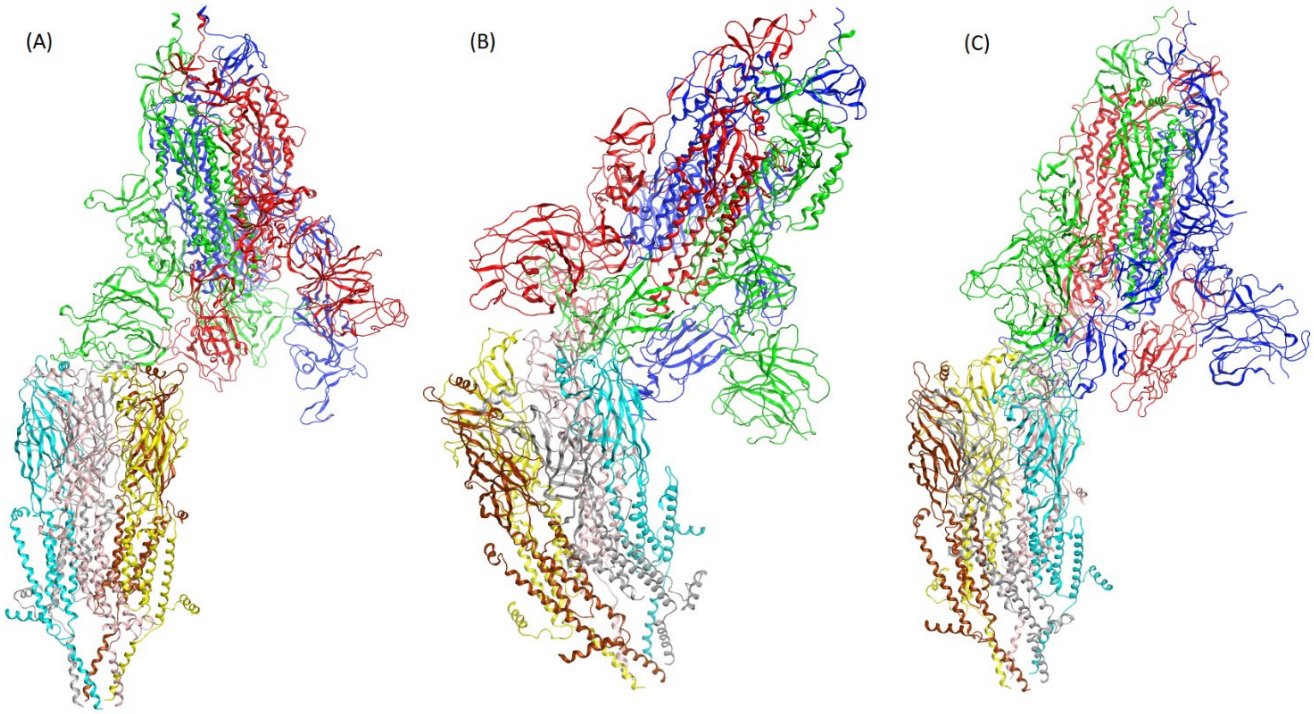


Figure 2. *α7* appears in the bottom region in complex with the (**A**) main spike, (**B**) Delta, and (**C**) Omicron variants of spike protein on top; Spike protein trimer is colored in dark blue (chain A), red (chain B), and green (chain C). The α7nAChr pentamer is colored in cyan (chain A), pink (chain B), yellow (chain C), brown (chain D), and gray (chain E). In (**A**), the chain B (pink) and chain C (yellow) monomers of the α7nAChr are interacting with the chain A (dark blue) and chain B (red) monomers of the main spike protein. In (**B**), the chain B (pink) and chain C (yellow) monomers of the α7nAChr are interacting with the chain C (green) and chain B (red) monomers of the Delta variant of spike protein. In (**C**), the chain B (pink) and chain C (yellow) parts of the α7nAChr are interacting with the chain A (dark blue) and chain C (green) monomers from the omicron variant of spike protein.

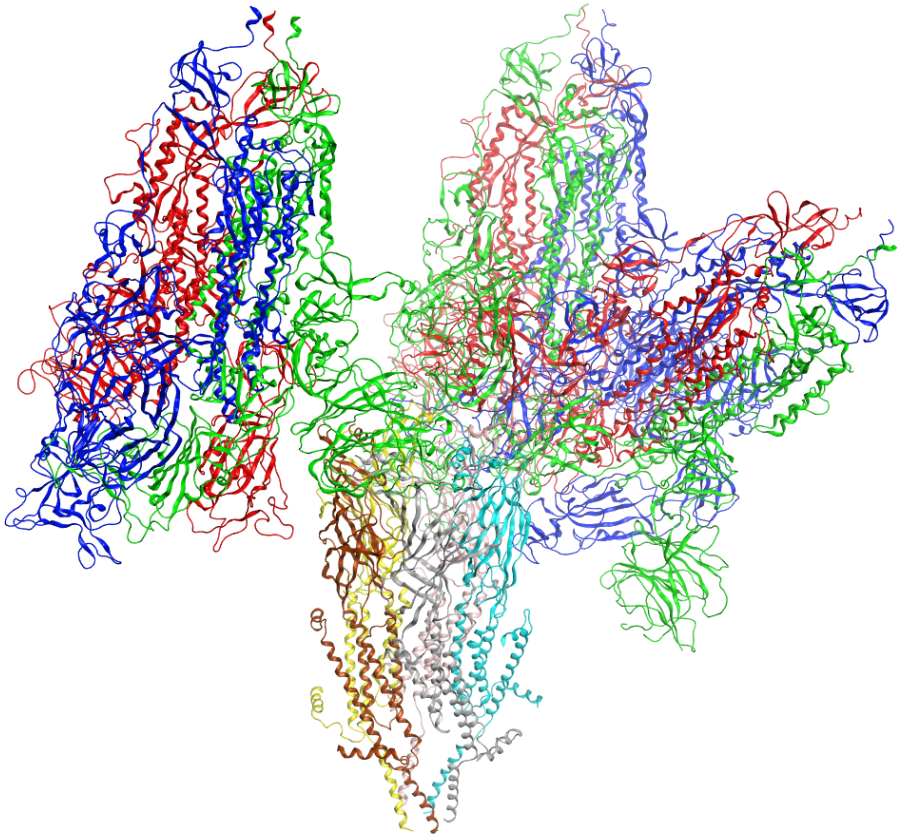


Figure 3. *α7* appears in the bottom region in the complex with the main spike on the left, Omicron in the middle, and the Delta variant on the right. The α7nAChr pentamer is colored in cyan (chain A), pink (chain B), yellow (chain C), brown (chain D), and gray (chain E). Regarding all the spikes we can see, chain A (dark blue), chain B (red), and chain C (green).

4. Discussion

Omicron, the latest SARS-CoV-2 variant, is spreading rapidly across the world, causing an unprecedented number of infections. The more rapid replication, when compared to the previous COVID-19 variants, and the higher number of novel mutations affecting the RBD and NTD of the spike protein (i.e., the primary sites targeted by naturally induced or vaccine-elicited neutralizing antibodies) allow Omicron to evade natural immunity, vaccines, and therapeutic antibodies. Regardless of the origin of these concerning genetic characteristics, both the clinical data from humans and the experimental data from animal models suggest that Omicron represents a less severe, more indolent form of infection [3–6]. Nevertheless, the biological factors underlying the decreased virulence of Omicron remain poorly understood. Strategies and methods performed in this study could potentially help predict how future variants will interact with different biological structures, depending on the amino-acids-mutation characteristics of the variant of interest.

In a previous study, through in silico analysis, we demonstrated the potential direct binding of the SARS-CoV-2 spike-1 protein to the Alpha-7 nicotinic acetylcholine receptor (α7nAChr), which is the core receptor under the control of the vagus nerve regulating the parasympathetic nervous system and the cholinergic anti-inflammatory pathway [12]. We also demonstrated strong binding by the macrocyclic lactone ivermectin and related compounds to the α7nAChr, while other studies have demonstrated that ivermectin acts as a positive allosteric effector of the α7nAChr [28,29]. This anti-inflammatory effect was identified as contributing to a significant reduction in the severity of clinical signs ($p < 0.001$) by concurrent ivermectin administration in golden hamsters intranasally inoculated with SARS-CoV-2 [30]. It has also recently been demonstrated that antibodies, such as human mAb CR3022 and COVA1–16 mAb, which binds the SARS-CoV-2 spike glycoprotein

specifically to the region targeting the conserved cryptic epitope on the spike glycoprotein that coincides with the toxin-like sequence interacting with the α7nAChr, have strong neutralizing properties against both SARS1 and COVID-19 [31,32]. One cannot overemphasize the importance of this binding in the pathophysiology of severe COVID infection, as dysautonomia-related symptoms (e.g., alterations in the respiratory rate, heartbeat, blood pressure, vessel tone, hormone secretion, intestinal peristalsis, digestion, etc.), uncontrolled inflammatory response (i.e., cytokine storm, which is mediated by α7nAChr-expressing alveolar macrophages and other cytokine-secreting cells, including histamine-secreting mast cells), and thromboembolic complications (i.e., the major causes of morbidity and mortality in infections caused by all previous COVID-19 variants) may all be attributable to the dysregulation of the nicotinic cholinergic system (NCS), as previously hypothesized [9–11].

If this hypothesis is correct, the attenuated nature of the Omicron infection in humans and animals, relative to previous variants, may be related to the acquisition of a set of genetic alterations specifically affecting the binding site of the SARS-CoV-2 spike-1 protein to the α7nAChr. To evaluate this possibility, we performed experiments using protein–ligand docking simulations to evaluate and compare the capacity of SARS-CoV-2 spike-1 proteins from the different COVID-19 variants (i.e., Alpha, Beta, Gamma, Delta, and Omicron) to bind to the human α7nAChr. As a notable contribution of the present work, we found that 10 of the 14 mutated residues on the RBD of the B.1.1.529 (Omicron) spike were located at the interface of the interaction with the α7nAChr, whereas no more than two mutated residues were present at this interface for any of the previous COVID-19 variants. More importantly, we found that these genetic alterations predict a dramatic decrease in the ability of Omicron SARS-CoV-2 spike-1 protein to bind to the α7nAChr, which, as noted above, is the core receptor regulating the parasympathetic nervous system and the cholinergic anti-inflammatory pathway.

Several clinical features of the Omicron infection are consistent with a decreased COVID-19 binding to the α7nAChr. For example, while the loss of smell (anosmia) and/or of taste (ageusia) have been considered hallmarks of all previous COVID-19 infection variants, and bearing in mind that the α7nAChr is highly expressed in human nerves, including the olfactory and gustatory nerves [33], only 0.17 percent of patients infected with Omicron have been reported to have developed anosmia [34]. Furthermore, the life-threatening cytokine storm (i.e., the severe immune reaction seen after 7–8 days from the onset of symptoms in the subset of patients developing severe COVID-19 infection) has been shown to be less prevalent in Omicron-infected patients, with a recent case series of 125 hospitalized Omicron-infected patients reporting 0 such cases [35]. These clinical data, combined with our results coming from protein–protein docking and relative to the energy states of the complexes, provide further support to the notion that, in addition to the experimentally proven inability of Omicron to reproduce in the lower airways [1,2], this variant may also have lost the ability to infect/inflame the α7nAChr overexpressing alveolar macrophages.

In conclusion, empirical results suggest that the Omicron spike-1 protein has acquired RBD mutations that, while they allow it to evade immunity from vaccines and the natural immunity afforded by previous infection, also confer a reduced capacity to bind to the α7nAChr, i.e., the main regulators of the brain cholinergic anti-inflammatory pathway [36]. Because the uncontrolled inflammatory response and other clinical symptoms of COVID-19 (e.g., anosmia and thromboembolic complications) may be caused by NCS dysregulation (9–11), this unique feature of Omicron may explain its intrinsically reduced virulence and account for the decreased risk of severe hospitalization or death associated with Omicron, compared to previous variants [37].

5. Conclusions

We used protein–ligand docking simulations to evaluate and compare the capacity of SARS-CoV-2 spike-1 proteins from the different COVID-19 variants to bind to the human α7nAChr. Our in silico results demonstrated that 10 out of the 14 mutated residues on the RBD of the B.1.1.529 (Omicron) spike, compared to between 0 and 2 in all previous variants, were present at the interface of the interaction with the α7nAChr. Importantly, we found that these genetic alterations caused a dramatic decrease in the ability of the Omicron SARS-CoV-2 spike-1 protein to bind to the α7nAChr. Because the α7nAChr is the core receptor under the control of the vagus nerve regulating the parasympathetic nervous system and the cholinergic anti-inflammatory pathway, and this anti-inflammatory pathway is known to play a crucial role in balancing the body's response to inflammation and sepsis, connecting the involuntary parasympathetic nervous system innervating all major organs to cytokine-producing cells, which in turn play a major role during the inflammatory phase of COVID-19 infection (i.e., the cytokine storm), we suggest that the attenuated nature of the Omicron infection in humans and animals, compared to previous variants, may be attributable to a particular set of genetic alterations, specifically affecting the binding site of the SARS-CoV-2 spike-1 protein to the α7nAChr.

Author Contributions: Conceptualization, A.D.S.; methodology, M.A. and D.D.; validation, M.A., D.E.S., A.D.S. and J.A.T.; formal analysis, D.D. and M.A.; investigation, D.D., A.D.S., D.E.S., J.A.T. and M.A.; resources, J.A.T.; data curation, D.D.; writing—original draft preparation, D.D., A.D.S. and D.E.S.; writing—review and editing, D.D., A.D.S., D.E.S., J.A.T. and M.A.; visualization, D.D.; supervision, M.A. and J.A.T.; project administration, M.A. and J.A.T. All authors have read and agreed to the published version of the manuscript.

Funding: This work was supported by the Natural Sciences and Engineering Research Council (NSERC) of Canada, grant RES00038219.

Institutional Review Board Statement: Not applicable.

Informed Consent Statement: Not applicable.

Data Availability Statement: The datasets used and analyzed in the current study are available from the corresponding author upon request.

Conflicts of Interest: A.D.S. reports grants from PUMA, grants from IMMUNOMEDICS, grants from GILEAD, grants from SYNTHON, grants and personal fees from MERCK, grants from BOEHINGER-INGELHEIM, grants from GENENTECH, grants and personal fees from TESARO and grants and personal fees from EISAI. The other authors declare no conflict of interest.

Abbreviations

The following abbreviations are used in this manuscript:

α7nAChr	Alpha-7 nicotinic acetylcholine receptor
COVID-19	Coronavirus disease 2019
IL-1	Interleukin 1
IL-6	Interleukin 6
MOE	Molecular Operating Environment
NTD	N-terminal domain
PDB	Protein Data Bank
RBD	Receptor binding domain
RMSD	Root mean square deviation
SARS-CoV-2	Severe acute respiratory syndrome coronavirus 2
SPR	Surface plasmon resonance
TNF	Tumor necrosis factor

References

1. McCallum, M.; Czudnochowski, N.; Rosen, L.E.; Zepeda, S.K.; Bowen, J.E.; Walls, A.C.; Hauser, K.; Joshi, A.; Stewart, C.; Dillen, J.R.; et al. Structural basis of SARS-CoV-2 Omicron immune evasion and receptor engagement. *Science* **2022**, *375*, 864–868. [CrossRef] [PubMed]
2. Hui, K.P.Y.; Ho, J.C.W.; Cheung, M.C.; Ng, K.C.; Ching, R.H.H.; Lai, K.L.; Kam, T.T.; Gu, H.; Sit, K.Y.; Hsin, M.K.Y.; et al. SARS-CoV-2 Omicron variant replication in human bronchus and lung ex vivo. *Nature* **2022**, *603*, 715–720. [CrossRef] [PubMed]
3. Maslo, C.; Toubkin, M. Characteristics and Outcomes of Hospitalized Patients in South Africa During the COVID-19 Omicron Wave-Reply. *JAMA* **2022**, *327*, 2148. [CrossRef] [PubMed]
4. Madhi, S.A.; Kwatra, G.; Myers, J.E.; Jassat, W.; Dhar, N.; Mukendi, C.K.; Nana, A.J.; Blumberg, L.; Welch, R.; Ngorima-Mabhena, N.; et al. Population Immunity and Covid-19 Severity with Omicron Variant in South Africa. *N. Engl. J. Med.* **2022**, *386*, 1314–1326. [CrossRef]
5. Wolter, N.; Jassat, W.; Walaza, S.; Welch, R.; Moultrie, H.; Groome, M.; Amoako, D.G.; Everatt, J.; Bhiman, J.N.; Scheepers, C.; et al. Early assessment of the clinical severity of the SARS-CoV-2 omicron variant in South Africa: A data linkage study. *Lancet* **2022**, *399*, 437–446. [CrossRef]
6. Bentley, E.G.; Kirby, A.; Sharma, P.; Kipar, A.; Mega, D.F.; Bramwell, C.; Penrice-Randal, R.; Prince, T.; Brown, J.C.; Zhou, J.; et al. SARS-CoV-2 Omicron-B.1.1.529 Variant leads to less severe disease than Pango B and Delta variants strains in a mouse model of severe COVID-19. *bioRxiv* **2021**. [CrossRef]
7. Shuai, H.; Chan, J.F.; Hu, B.; Chai, Y.; Yuen, T.T.; Yin, F.; Huang, X.; Yoon, C.; Hu, J.C.; Liu, H.; et al. Attenuated replication and pathogenicity of SARS-CoV-2 B.1.1.529 Omicron. *Nature* **2022**, *603*, 693–699. [CrossRef]
8. Abdelnabi, R.; Foo, C.S.; Zhang, X.; Lemmens, V.; Maes, P.; Slechten, B.; Raymenants, J.; André, E.; Weynand, B.; Dallmeier, K.; et al. The omicron (B.1.1.529) SARS-CoV-2 variant of concern does not readily infect Syrian hamsters. *Antivir. Res.* **2022**, *198*, 105253. [CrossRef] [PubMed]
9. Aminpour, M.; Cannariato, M.; Safaeeardebili, M.E.; Preto, J.; Moracchiato, A.; Doria, D.; Donato, F.; Zizzi, E.A.; Deriu, M.A.; Scheim, D.E.; et al. In Silico Analysis of the Multi-Targeted Mode of Action of Ivermectin and Related Compounds. *Computation* **2022**, *10*, 51. [CrossRef]
10. Changeux, J.P.; Amoura, Z.; Rey, F.A.; Miyara, M. A nicotinic hypothesis for Covid-19 with preventive and therapeutic implications. *Comptes Rendus Biol.* **2020**, *343*, 33–39.
11. Lagoumintzis, G.; Chasapis, C.T.; Alexandris, N.; Kouretas, D.; Tzartos, S.; Eliopoulos, E.; Farsalinos, K.; Poulas, K. Nicotinic cholinergic system and COVID-19: In silico identification of interactions between alpha7 nicotinic acetylcholine receptor and the cryptic epitopes of SARS-Co-V and SARS-CoV-2 Spike glycoproteins. *Food Chem. Toxicol.* **2021**, *149*, 112009. [CrossRef] [PubMed]
12. Wang, H.; Yu, M.; Ochani, M.; Amella, C.A.; Tanovic, M.; Susarla, S.; Li, J.H.; Wang, H.; Yang, H.; Ulloa, L.; et al. Nicotinic acetylcholine receptor α7 subunit is an essential regulator of inflammation. *Nature* **2003**, *421*, 384–388. [CrossRef] [PubMed]
13. Oliveira, A.S.F.; Ibarra, A.A.; Bermudez, I.; Casalino, L.; Gaieb, Z.; Shoemark, D.K.; Gallagher, T.; Sessions, R.B.; Amaro, R.E.; Mulholland, A.J. A potential interaction between the SARS-CoV-2 spike protein and nicotinic acetylcholine receptors. *Biophys. J.* **2021**, *120*, 983–993. [CrossRef] [PubMed]
14. Daly, J.L.; Simonetti, B.; Klein, K.; Chen, K.-E.; Williamson, M.K.; Antón-Plágaro, C.; Shoemark, D.K.; Simón-Gracia, L.; Bauer, M.; Hollandi, R.; et al. Neuropilin-1 is a host factor for SARS-CoV-2 infection. *Science* **2020**, *370*, 861–865. [CrossRef] [PubMed]
15. Walls, A.C.; Park, Y.-J.; Tortorici, M.A.; Wall, A.; McGuire, A.T.; Veesler, D. Structure, Function, and Antigenicity of the SARS-CoV-2 Spike Glycoprotein. *Cell* **2020**, *181*, 281-292.e6. [CrossRef]
16. Davidson, A.D.; Williamson, M.K.; Lewis, S.; Shoemark, D.; Carroll, M.W.; Heesom, K.J.; Zambon, M.; Ellis, J.; Lewis, P.A.; Hiscox, J.A.; et al. Characterisation of the transcriptome and proteome of SARS-CoV-2 reveals a cell passage induced in-frame deletion of the furin-like cleavage site from the spike glycoprotein. *Genome Med.* **2020**, *12*, 68. [CrossRef]
17. Ren, C.; Tong, Y.L.; Li, J.C.; Lu, Z.Q.; Yao, Y.M. The Protective Effect of Alpha 7 Nicotinic Acetylcholine Receptor Activation on Critical Illness and Its Mechanism. *Int. J. Biol. Sci.* **2017**, *13*, 46–56. [CrossRef]
18. Gahring, L.C.; Myers, E.J.; Dunn, D.M.; Weiss, R.B.; Rogers, S.W. Nicotinic alpha 7 receptor expression and modulation of the lung epithelial response to lipopolysaccharide. *PLoS ONE* **2017**, *12*, e0175367. [CrossRef]
19. Zhao, X.; Yu, Z.; Lv, Z.; Meng, L.; Xu, J.; Yuan, S.; Fu, Z. Activation of Alpha-7 Nicotinic Acetylcholine Receptors (α7nAchR) Promotes the Protective Autophagy in LPS-Induced Acute Lung Injury (ALI) In Vitro and In Vivo. *Inflammation* **2019**, *42*, 2236–2245. [CrossRef]
20. Fajgenbaum, D.C.; June, C.H. Cytokine Storm. *N. Engl. J. Med.* **2020**, *383*, 2255–2273. [CrossRef]
21. Lentz, T.L.; Burrage, T.G.; Smith, A.L.; Crick, J.; Tignor, G.H. Is the acetylcholine receptor a rabies virus receptor? *Science* **1982**, *215*, 182–184. [CrossRef]
22. Courties, A.; Boussier, J.; Hadjadj, J.; Yatim, N.; Barnabei, L.; Péré, H.; Veyer, D.; Kernéis, S.; Carlier, N.; Pène, F.; et al. Regulation of the acetylcholine/α7nAChR anti-inflammatory pathway in COVID-19 patients. *Sci. Rep.* **2021**, *11*, 11886. [CrossRef]
23. Noviello, C.M.; Gharpure, A.; Mukhtasimova, N.; Cabuco, R.; Baxter, L.; Borek, D.; Sine, S.M.; Hibbs, R.E. Structure and gating mechanism of the α7 nicotinic acetylcholine receptor. *Cell* **2021**, *184*, 2121-2134.e13. [CrossRef]
24. Ni, D.; Lau, K.; Turelli, P.; Raclot, C.; Beckert, B.; Nazarov, S.; Pojer, F.; Myasnikov, A.; Stahlberg, H.; Trono, D. Structural analysis of the Spike of the Omicron SARS-COV-2 variant by cryo-EM and implications for immune evasion. *bioRxiv* **2021**. [CrossRef]

25. Wang, Y.; Liu, C.; Zhang, C.; Wang, Y.; Hong, Q.; Xu, S.; Li, Z.; Yang, Y.; Huang, Z.; Cong, Y. Structural basis for SARS-CoV-2 Delta variant recognition of ACE2 receptor and broadly neutralizing antibodies. *Nat. Commun.* **2022**, *13*, 871. [CrossRef]
26. Duhovny, D.; Nussinov, R.; Wolfson, H.J. *Efficient Unbound Docking of Rigid Molecules*; Springer: Berlin/Heidelberg, Germany, 2002; pp. 185–200.
27. Schneidman-Duhovny, D.; Inbar, Y.; Nussinov, R.; Wolfson, H.J. PatchDock and SymmDock: Servers for rigid and symmetric docking. *Nucleic Acids Res.* **2005**, *33*, W363–W367. [CrossRef]
28. Krause, R.M.; Buisson, B.; Bertrand, S.; Corringer, P.J.; Galzi, J.L.; Changeux, J.P.; Bertrand, D. Ivermectin: A positive allosteric effector of the alpha7 neuronal nicotinic acetylcholine receptor. *Mol. Pharmacol.* **1998**, *53*, 283–294. [CrossRef]
29. Zemkova, H.; Tvrdonova, V.; Bhattacharya, A.; Jindrichova, M. Allosteric modulation of ligand gated ion channels by ivermectin. *Physiol. Res.* **2014**, *63* (Suppl. 1), S215–S224. [CrossRef]
30. de Melo, G.D.; Lazarini, F.; Larrous, F.; Feige, L.; Kornobis, E.; Levallois, S.; Marchio, A.; Kergoat, L.; Hardy, D.; Cokelaer, T.; et al. Attenuation of clinical and immunological outcomes during SARS-CoV-2 infection by ivermectin. *EMBO Mol. Med.* **2021**, *13*, e14122.
31. Yuan, M.; Wu, N.C.; Zhu, X.; Lee, C.D.; So, R.T.Y.; Lv, H.; Mok, C.K.P.; Wilson, I.A. A highly conserved cryptic epitope in the receptor binding domains of SARS-CoV-2 and SARS-CoV. *Science* **2020**, *368*, 630–633. [CrossRef]
32. Liu, H.; Wu, N.C.; Yuan, M.; Bangaru, S.; Torres, J.L.; Caniels, T.G.; van Schooten, J.; Zhu, X.; Lee, C.D.; Brouwer, P.J.M.; et al. Cross-Neutralization of a SARS-CoV-2 Antibody to a Functionally Conserved Site Is Mediated by Avidity. *Immunity* **2020**, *53*, 1272-1280.e5. [CrossRef] [PubMed]
33. D'Souza, R.D.; Vijayaraghavan, S. Paying attention to smell: Cholinergic signaling in the olfactory bulb. *Front. Synaptic Neurosci.* **2014**, *6*, 21. [PubMed]
34. Coelho, D.H.; Reiter, E.R.; French, E.; Costanzo, R.M. Decreasing Incidence of Chemosensory Changes by COVID-19 Variant. *Otolaryngol. Head Neck Surg.* **2022**, 1945998221097656. [CrossRef] [PubMed]
35. Debroy, S. Severe Immune Effect Seen in Delta Absent in Omicron Cases in Mumbai: City Hospital Data. Times of India, 17 January 2022. Available online: https://timesofindia.indiatimes.com/city/mumbai/severe-immune-effect-seen-in-delta-absent-in-omicron-city-hosp-data/articleshow/88939499.cms (accessed on 5 September 2022).
36. Piovesana, R.; Salazar Intriago, M.S.; Dini, L.; Tata, A.M. Cholinergic Modulation of Neuroinflammation: Focus on alpha7 Nicotinic Receptor. *Int. J. Mol. Sci.* **2021**, *22*, 4912. [CrossRef]
37. Davies, M.A.; Kassanjee, R.; Rousseau, P.; Morden, E.; Johnson, L.; Solomon, W.; Hsiao, N.Y.; Hussey, H.; Meintjes, G.; Paleker, M.; et al. Outcomes of laboratory-confirmed SARS-CoV-2 infection in the Omicron-driven fourth wave compared with previous waves in the Western Cape Province, South Africa. *Trop. Med. Int. Health* **2022**, *27*, 564–573. [CrossRef]